PHYSICAL REVIEW A **81**, 030501(R) (2010)

Quantifying the strength and asymmetry of giant resonances in the photorecombination of Sc^{3+} and the photoionization of Sc^{2+}

D. Nikolić and T. W. Gorczyca
Western Michigan University, Kalamazoo, Michigan 49008, USA

N. R. Badnell
University of Strathclyde, Glasgow G4 0NG, United Kingdom

(Received 9 November 2009; published 5 March 2010)

We report on strong interference effects for the dominant, highly correlated, broad, and asymmetric $3p^5 3d^2(^2F^o_{5/2,7/2})$ giant resonances in the photorecombination of Sc^{3+}. Using a nonorthogonal perturbative multiconfiguration Breit-Pauli approach, we present theoretical photorecombination cross sections that are in line with the Test Storage Ring measurements of Schippers *et al.* In order to reproduce the observed asymmetric resonance profiles near threshold, it was necessary to include resonance-continuum interference. Also, we present Sc^{2+} photoionization cross sections that agree with the Advance Light Source measurements of Schippers *et al.* This perturbative method is based on analytical expressions for the cross sections in terms of computed energies and transition rates, thereby directly determining resonance strengths and Fano asymmetry parameters. Of particular note, our reported absolute cross sections are in excellent agreement with experimental results, in contrast to all previous theoretical calculations. Furthermore, the apparent violation of the sum rule prediction, determined both from our integrated photoionization cross sections and from experimental results, is found to be due to radiative damping of narrow resonances.

DOI: 10.1103/PhysRevA.81.030501 PACS number(s): 31.15.vj, 34.80.Lx, 32.80.Zb

Electron-ion photorecombination (PR) of low-charged Sc ions is of interest for understanding the diverse ambient plasmas found in laboratory [1] and astrophysical [2,3] environments. However, there are few experimental or theoretical studies on PR of low-charged M-shell ions, perhaps due to the complex nature of these systems. Experimentally, the low charge-to-mass ratio makes it difficult to obtain high resolution. Theoretically, on the other hand, third-row systems, with their nearly filled $n = 3$ shells, are notoriously difficult to describe accurately because of the huge amount of configuration-interaction required.

However, experimental cross sections have been determined for Sc^{3+} PR [4] and the reverse process of Sc^{2+} photoionizaion (PI) [5], which proceeds schematically as

$$\begin{array}{ccccc} e^- + \mathrm{Sc}^{3+}(3p^6) & \longrightarrow & \mathrm{Sc}^{2+**}\begin{pmatrix} 3p^5 3d n\ell \\ 3p^5 4s n\ell \end{pmatrix} & & \\ & \overset{\mathrm{RR}}{\searrow} & \overset{\mathrm{DR}}{\downarrow} & & \\ & & \mathrm{Sc}^{2+*}(3p^6 n\ell) + \hbar\omega. & & \end{array} \quad (1)$$

For Sc^{3+} PR, the dominant dielectronic recombination (DR) process consists of an initial electron-ion continuum state c that captures dielectronically into an intermediate doubly excited Sc^{2+**} autoionizing state d, which then decays radiatively to a Sc^{2+*} bound state b, in competition with the direct radiative recombination (RR). PI of Sc^{2+} is simply the reverse process of Eq. (1) from just the $3p^6 3d$ ground state. RR and DR transition amplitudes add coherently, giving rise in general to asymmetric, Fano resonance profiles [6], which we quantify with asymmetry parameters $Q^d_{c\to b}$ given in Table I.

Previous theoretical and experimental investigations of Sc^{2+} PI [5,7,8] and Sc^{3+} PR [4,9] have been in agreement for the qualitative nature of the asymmetric $3p^5 3d^2(^2F)$ resonance features, but all theoretical cross sections for the resonance strength [4,7–9] have been roughly 60% larger than the measured cross sections [4,5]. Since the absolute experimental Sc^{2+} PI cross section [5] was normalized to the experimental Sc^{3+} PR cross section [4] for the strong $3p^5 3d^2(^2F)$ super-Coster-Kronig resonance region via the principle of detailed balance, the outstanding puzzle is whether the experimental PR cross section is about 2/3 too low or all previous theoretical results are ≈60% too high. The matter is complicated by the unexplained apparent violation of the Thomas-Reiche-Kuhn sum rule [10] raised by Sossah *et al.* [8] that their integrated PI cross section gave a total oscillator strength of 5.29, in accord with the sum rule prediction of 6.0, whereas the experimental *ionization* cross section gave a value of 3.24. This apparent violation is explained below as due to radiation damping of narrow $3p^5 3d n\ell$ and $3p^5 4s n\ell$ resonances, resulting in a branching of the absorption strength into 60% ionization and 40% radiative stabilization channels. Thus the measured ionization oscillator strength should be only about 60% of the sum rule prediction of 6.0.

In order to address the outstanding discrepancy between the calculated and experimental resonance strengths, we first studied the entire Sc^{3+} and Ti^{4+} PR spectra [11] using the atomic structure and collision code AUTOSTRUCTURE [12]—a multiconfiguration Breit-Pauli (MCBP) approach within an independent-processes, isolated-resonance approximation. The main issue addressed in Ref. [11] was the effect of external fields on the Rydberg series of $3p^5 3d(n \geqslant 14)\ell$ resonances observed in Sc^{3+} PR at about 42 eV. Due to the large discrepancies in resonance positions, however, it was clear that a more-converged theoretical description of the $3p^5 3d(n = 3, 4)\ell$ resonances was required. Those initial calculations were then improved by using a highly correlated

TABLE I. Energies [relative to the $Sc^{3+}3p^6(^1S_0)$ ground state] and radiative data for dominant transitions for the Sc^{3+} target states (top), final bound states (middle), and interfering autoionizing resonances (bottom). Resonant states are labeled according to Fig. 1 and assume a closed-shell Mg-like core.

Sc^{3+}			Energy (Ry)		
Config.	Level	$K_{(\%)}$	Present[a]	MCHF[b]	NIST[c]
$3p^6$	$^1S_0$	$1_{(100)}$	0.00000	0.00000	0.00000
$3p^53d$	$^3P^o_0$	$2_{(99.7)}$	2.18782	2.07342	2.18452
$3p^53d$	$^3P^o_1$	$3_{(99.4)}$	2.19492	2.07966	2.19071
$3p^53d$	$^3P^o_2$	$4_{(98.7)}$	2.20933	2.09204	2.20357
$3p^53d$	$^3F^o_4$	$5_{(100)}$	2.27197	2.17668	2.28462
$3p^53d$	$^3F^o_3$	$6_{(97.8)}$	2.28784	2.18865	2.29738
$3p^53d$	$^3F^o_2$	$7_{(97.7)}$	2.30296	2.19971	2.30920
$3p^53d$	$^3D^o_3$	$8_{(62.5)}$; $12_{(37.5)}$	2.41752	2.33926	2.44251
$3p^53d$	$^1D^o_2$	$9_{(57.6)}$; $11_{(40.1)}$	2.42852	2.33411	2.43695
$3p^53d$	$^3D^o_1$	$10_{(99.6)}$	2.43838	2.35094	2.45519
$3p^53d$	$^3D^o_2$	$11_{(58.4)}$; $9_{(40.7)}$	2.44159	2.35114	2.45550
$3p^53d$	$^1F^o_3$	$12_{(61.2)}$; $8_{(36.6)}$	2.44599	2.36733	2.47004
$3p^54s$	$^3P^o_2$	$13_{(99.7)}$	3.00254	2.92088	3.03535
$3p^54s$	$^3P^o_1$	$14_{(86.1)}$; $17_{(11.9)}$	3.02473	2.93460	3.04732
$3p^54s$	$^3P^o_0$	$15_{(99.7)}$	3.04761	2.95754	3.07407
$3p^53d$	$^1P^o_1$	$16_{(58.1)}$; $17_{(31.8)}$; $14_{(10.1)}$	3.06914	2.96776	3.07538
$3p^54s$	$^1P^o_1$	$17_{(56.3)}$; $16_{(40.1)}$; $14_{(3.6)}$	3.11880	3.06976	3.14392

Radiative transition	A^r (ns^{-1})	S (a.u.)	f_ℓ	f_v
$3p^6(^1S_0) \rightarrow K = 17\ (^1P^o_1)$	102.4[a]	3.780[a]	3.93[a]	3.41[a]
	126.3[c,d]	3.750[c,d]	3.93[c,d]	
	67.13[b]	2.600[b]	2.66[b]	

Sc^{2+}			Energy (Ry)	
Config.	Level	Label$_{(\%)}$	Present[a]	Experiment
$3p^63d$	$^3D_{3/2}$	$b_{1(100)}$	−1.81926	−1.81959[c]
$3p^63d$	$^3D_{5/2}$	$b_{2(100)}$	−1.81581	−1.81779[c]
$3p^53d^2$	$^2F^o_{5/2}$	$d_{1(97.5)}$	0.85360	0.9044(19)[e,f]
$3p^53d^2$	$^2F^o_{7/2}$	$d_{2(95.8)}$	0.86835	0.9099(2)[g,f]

Radiative transition	Label	A^r (ns^{-1})	S (a.u.)	f
$3p^63d(^2D_{3/2}) \rightarrow 3p^53d^2\ (^2F^o_{5/2})$	$b_1 \rightarrow d_1$	35.51[a]	4.167[a]	0.928[a]
$3p^63d(^2D_{5/2}) \rightarrow 3p^53d^2\ (^2F^o_{5/2})$	$b_2 \rightarrow d_1$	1.88[a]	0.221[a]	0.033[a]
$3p^63d(^2D_{5/2}) \rightarrow 3p^53d^2\ (^2F^o_{7/2})$	$b_2 \rightarrow d_2$	37.75[a]	5.816[a]	0.868[a]

Autoionizing transition or label	$A^a_{d\rightarrow c}$ (fs^{-1})	Label	$Q^d_{c\rightarrow b}$
$3p^53d^2(^2F^o_{5/2}) \rightarrow 3p^6\epsilon f(^2F^o_{5/2})$	1.555[a]	$c \xrightarrow{d_1} b_1$	6.05[a]
$d_1 \rightarrow c$	1.272[h]	$c \xrightarrow{d_1} b_2$	−5.14[a]
	$1.35_{(10)}$[e,f]		
$3p^53d^2(^2F^o_{7/2}) \rightarrow 3p^6\epsilon f(^2F^o_{7/2})$	1.568[a]	$c \xrightarrow{d_2} b_2$	5.97[a]
$d_2 \rightarrow c$	1.295[h]		6.36[e,f]
	$1.287_{(8)}$[g,f]		$5.02_{(8)}$[g,f]

[a]Present perturbative MCBP calculations (using 17 levels for Sc^{3+} and 594 levels for Sc^{2+}).
[b]Multiconfiguration Hartree-Fock (theoretical) [14].
[c]NIST (experimental) [15].
[d]Assigned experimental uncertainty: $\leqslant 18\%$.
[e]TSR (experimental, PR of Sc^{3+}) [4].
[f]Fit of unresolved $3p^53d^2(^2F^o)$ resonances.
[g]ALS (experimental, PI of Sc^{2+}) [5].
[h]BP R-matrix (theoretical, PI of Sc^{2+}) [8].

atomic basis for Ti^{4+} PR [13], giving excellent agreement with the experimental results [4]. Our main objective in the present study is to apply those same methods to Sc^{3+} PR for the energy region containing the broad, asymmetric $3p^53d^2(^2F)$ resonances, hereafter denoted as $d_{1,2}$, and their neighboring perturbers, thereby obtaining absolute resonance cross sections that are in excellent agreement with experiment; moreover, by resolving the discrepancy between earlier theoretical works and experiment, we explain the apparent violation of the sum rule as being due to radiative damping of narrow resonances.

We use the exact same theoretical approach as was given in detail in our previous work on isoelectronic argon-like Ti^{4+} PR [13]. Briefly, a MCBP method is employed that includes single, double, and triple promotions out of the target, resonance, and bound configurations listed in Table I and also includes the dominant relativistic effects such as the spin-orbit interaction. Higher-order resonance-continuum and resonance-resonance interference effects are also considered. Of particular utility, a basis of nonorthogonal orbitals is used where a unique set is optimized for each target, resonance, and bound state, thereby incorporating important term-dependent and relaxation effects. Our earlier work on PR of Mg^{2+} [16] and Ti^{4+} [13] demonstrated that such a nonorthogonal basis yields accurate energies and transition rates for highly sensitive cases.

Our computed excitation energies and the dominant radiative transition quantities for Sc^{2+} and Sc^{3+} are given in Table I, along with other theoretical and experimental results, showing agreement to better than 1% with the NIST values. For the ground $b_{1,2}$ and resonant $d_{1,2}$ states, reasonable agreement is found with TSR [4] and ALS [5] experimental results. Namely, our theoretical widths and line strengths for the dominant $d_{1,2}$ resonances are about 15 and 22% larger than those observed in the TSR and ALS experiments, respectively, while the computed positions are about 6% lower than the experimental TSR values.

The BPRM approach of Sossah *et al.* [8], using orthogonal orbitals, gave resonance positions and widths in better agreement with the ALS experimental values than our MCBP results. However, their integrated oscillator strength for the dominant resonance region is 5.29, in approximate accord with the Thomas-Reiche-Kuhn summed oscillator value of 6.0 for the six active orbitals in the initial $3p^6$ ground-state configuration, whereas the integrated strength determined from the ALS PI spectrum was only 3.24 and therefore the experimental absolute normalization might be incorrect.

In our present comparison, it is interesting to note that the combined oscillator strength for the $K = 1 \rightarrow K = 16$ and $K = 1 \rightarrow K = 17$ radiative transitions in Sc^{3+} amounts to 5.30, as opposed to the total value of 5.29 computed by Sossah *et al.* [8] and attributed solely to $3p \rightarrow 3d$ promotion. Thus, in our calculations, due to a redistribution of the intra- and intershell oscillator strengths, only ∼74% of the many-body Thomas-Reiche-Kuhn sum rule [10] is exhausted by the $K = 1 \rightarrow K = 17$ core excitation. Consequently, the integrated strengths of Sc^{2+} resonances attached to this threshold should be ∼26% weaker compared to the Breit-Pauli R-matrix (BPRM) results of Sossah *et al.* [8].

It should be noted that, except for the two $d_{1,2}$ resonances, all computed $3p^53d^2$ and $3p^53d4s$ resonance positions found

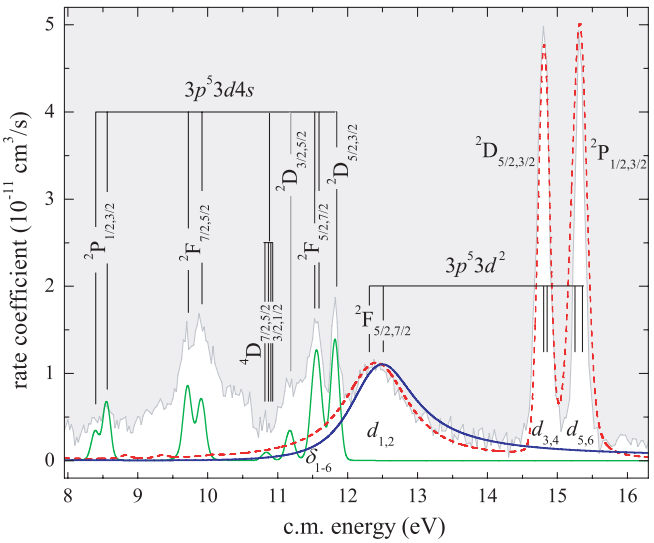

FIG. 1. (Color online) Comparison of the TSR measured Sc^{3+} PR rate coefficient [4] (white area) with the present lowest-order, perturbative MCBP results in the region of the $3p^5 3d4s$ (solid green curve) and $3p^5 3d^2$ (dashed red curve) resonances. The theoretically-designated $d_{1,2}$ resonances required an artificial shift by 0.691 eV to higher c.m. energies in order to align well with the measured spectra. The broad $d_{1,2}$ resonances (solid blue curve) are also described to next-highest order, thereby including DR/RR interference effects.

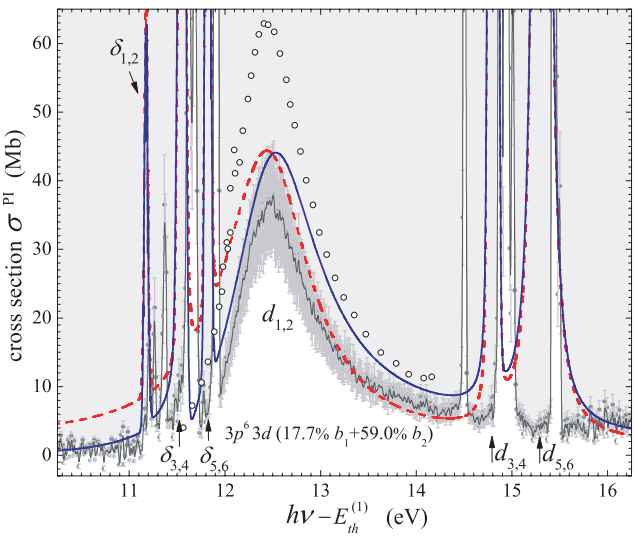

FIG. 2. (Color online) Comparison between computed and experimental PI cross sections for Sc^{2+}. Red dashed curve: present theoretical PI cross sections in lowest order, convoluted with the experimental energy spread of 44 meV. Blue solid curve: higher-order MCBP results including resonance-continuum interference effects. Open circles: segment of the PI cross section computed by Sossah *et al.* [8] in the vicinity of the $d_{1,2}$ resonances; (black points with dark gray error bars) high-resolution merged photon-ion beams experimental data of Schippers *et al.* [5]. The background areas below and above the experimental data are shaded as white and light gray, respectively, to show more clearly the high narrow experimental resonances in the 11- to 12-eV and 14.5- to 15.5-eV regions. The energy scale is given relative to the first ionization threshold $E_{th}^{(1)} = 24.75684$ eV.

in Fig. 1 are in excellent agreement with experiment and do not require an artificial energy shift, in contrast to the results reported in Ref. [11]. Furthermore, the two $d_{1,2}$ resonance positions are found to be 0.691 eV lower than the experimental values and are therefore shifted to higher energy by +0.691 eV—a significant improvement over the shift of −3.95 eV required in Ref. [11]. As this artificial shift is only a fraction of the broad $d_{1,2}$ resonance widths, coupling to the nearby $3p^5 3d4s$ resonances is restored by using the full expression for the PR cross section (see Eq. 9 in Ref. [13]). We note that the $d_{5,6}$ resonances located at 15.25 and 15.35 eV have widths of 88 and 76 meV, respectively, that are about 4 times larger than the observed PI widths [5], but that their computed strengths match the experimental PR value [4] rather well (see Fig. 1). Furthermore, they are distant enough from the asymmetric $d_{1,2}$ resonances not to influence their profile shape, which is not the case for the nearby δ_{1-6} resonances belonging to the $3p^5 3d4s$ configuration.

Our investigation of Sc^{2+} PI requires cross sections from each bound state $b_{1,2}$ to the pertinent $d_{1,2}$ resonances. Thus, we must retain all those states with computed energies of 11–16 eV. For this purpose, the lower portion of Table I lists our calculated parameters (see Eqs. (5)–(8) in Ref. [13]) for partial radiative A_d^r and autoionizing $A_{d\to c}^a$ transition rates between the ground $b_{1,2}$ and the resonant $d_{1,2}$ states in Sc^{2+}. Also, in order to compare detailed theoretical and experimental resonance profiles, and quantify resonant-direct (DR/RR) interference effects, Table I also gives the values for the asymmetry parameters $Q_{c\to b}^d$ (as defined by Eq. (11) of Ref. [13]) for $d_{1,2}$ resonances. The present results are in good agreement with both TSR [4] and ALS [5] measurements.

Theoretical PI cross sections are trivially inferred from our computed partial PR cross section using the principle of detailed balance, as previously done for isoelectronic Ti^{4+} [13]. Figure 2 shows present lowest-order (no resonance-continuum interference), next-highest-order (with interference), and experimental ALS [5] PI cross sections. It is seen that inclusion of the (finite) asymmetry parameters $Q_{c\to b}^d$ from Table I results in slightly shifted (∼0.1 eV) and asymmetric $d_{1,2}$ resonance profiles, as also observed experimentally, in contrast to the IPIRDW symmetric Lorentzian profiles. It is also important to note that the strength of the PI cross section is a sensitive function of the fractional abundances for Sc^{2+} metastable states and that we used $\eta_{3/2} = 0.177$ for ground b_1 and $\eta_{5/2} = 0.59$ for metastable b_2 states as reported in the ALS study [5]. The evident agreement, in both asymmetry and overall cross section, near the broad $d_{1,2}$ resonances, between the higher-order MCBP results and the measured cross section indicates that we have established an adequate theoretical description of the PR and inverse PI processes.

The present results are in accord with the ALS results, and the experimental integrated oscillator strength is only 3.24, much lower than the Thomas-Reiche-Khun sum rule value of 6.0 or the BPRM result of 5.29, as reported by Sossah *et al.* [8]. It might therefore seem that the present method does not account for all of the oscillator strength. However, we have mentioned previously that our total *absorption* oscillator strength sum is 5.30.

The missing oscillator strength in the ALS experiment is explained as follows. Resonant photoabsorption from the $3p^6 3d(^2D)$ ground state leads primarily to photoexcited $3p^6 3d^2$ and $3p^5 3d4s$ resonances that subsequently decay. In addition to the autoionization final channels, giving Sc^{3+} production, as observed experimentally, there are also radiative decay channels to ground or excited states. Of the 28 possible LS coupled states belonging to the $3p^5 3d^2$ and $3p^5 3d4s$ configurations, only 10 of these are allowed to autoionize within an LS coupling scheme, and the remaining 18 LS states decay primarily via radiative stabilization. However, their absorption strength can be significant, given their overlapping, and therefore mixing, with the strong $d_{1,2}$ resonances. This radiative channel is not measured and is not computed in our formulation, in which radiative decay reductions to the cross section are easily accounted for. The BPRM calculations, as implemented by Sossah *et al.* [8], did not include radiation damping effects but may not have resolved these extremely narrow resonances (the autoionization rate is much less than the radiative rate). The present calculations find that only about 60% of all the resonance absorption strength contributes to the PI cross section, with the remaining ≈40% going into radiative channels. However, we expect that newly developed experimental techniques [17] will provide more complete radiative data from EBIT via simultaneous detection of several charge-state selective DR and x-ray spectra.

In conclusion, we have successfully reproduced most of the main features observed in the TSR Sc^{3+} PR and ALS Sc^{2+} PI experiments. Detailed balance ensures that our two calculations are consistent, and they agree in strength with both TSR and the inverse ALS results, validating the experimental normalization in both measurements. As a further utility of this MCBP method, when extended to include resonance-interference effects, by using computed energies and rates within an analytic expression, Fano asymmetry parameters are determined that compare favorably with both experimental results for the strong, broad $3p^5 3d^2(^2F)$ resonances. Most importantly, our computed Sc^{3+} PR and Sc^{2+} PI absolute cross sections are in excellent agreement with TSR and ALS experimental results, respectively, in contrast to all previous theoretical results [4,8,9] that were ≈60% greater in magnitude.

We thank S. Schippers for providing us with the experimental data. This work was supported in part by NASA APRA and SHP SR&T programs.

[1] M. Martins, K. Godehusen, T. Richter, P. Wernet, and P. Zimmermann, J. Phys. B **39**, R79 (2006).
[2] F. Leblanc and G. Alecian, Astron. Astrophys. **477**, 243 (2008).
[3] H. W. Zhang, T. Gehren, and G. Zhao, Proc. Int. Astron. Union **4**, 127 (2008).
[4] S. Schippers, S. Kieslich, A. Müller, G. Gwinner, M. Schnell, A. Wolf, A. Covington, M. E. Bannister, and L. B. Zhao, Phys. Rev. A **65**, 042723 (2002).
[5] S. Schippers, A. Müller, S. Ricz, M. E. Bannister, G. H. Dunn, A. S. Schlachter, G. Hinojosa, C. Cisneros, A. Aguilar, A. M. Covington *et al.*, Phys. Rev. A **67**, 032702 (2003).
[6] U. Fano and J. W. Cooper, Phys. Rev. **137**, A1364 (1965).
[7] Z. Altun, S. Tokdemir, and S. T. Manson, Bull. Am. Phys. Soc. **41**, 1116 (1996).
[8] A. M. Sossah, H.-L. Zhou, and S. T. Manson, Phys. Rev. A **78**, 053405 (2008).
[9] T. W. Gorczyca, M. S. Pindzola, F. Robicheaux, and N. R. Badnell, Phys. Rev. A **56**, 4742 (1997).
[10] J. Krause, Lett. Nuovo Cimento **7**, 611 (1973).
[11] D. Nikolić, T. W. Gorczyca, J. Fu, D. W. Savin, and N. R. Badnell, Nucl. Instrum. Methods B **261**, 145 (2007).
[12] N. R. Badnell, J. Phys. B **19**, 3827 (1986); **30**, 1 (1997).
[13] D. Nikolić, T. W. Gorczyca, and N. R. Badnell, Phys. Rev. A **79**, 012703 (2009).
[14] A. Irimia and C. Froese-Fischer (2003), www.vuse.vanderbilt.edu/∼cff/mchf_collection.
[15] T. Shirai, J. Sugar, A. Musgrove, and W. L. Wiese, J. Phys. Chem. Ref. Data Monogr. **8**, 1 (2000).
[16] J. Fu, T. W. Gorczyca, D. Nikolić, N. R. Badnell, D. W. Savin, and M. F. Gu, Phys. Rev. A **77**, 032713 (2008).
[17] I. Orban, S. Tashenov, F. Ferro, E. Lindroth, and R. Schuch (submitted to Phys. Rev. Lett. 2009).